Synthesis and Morphology of Well-Defined Poly(ethylene-*co*-acrylic acid) Copolymers

Travis W. Baughman,[†] Christopher D. Chan,[‡] Karen I. Winey,*[,§] and Kenneth B. Wagener*[,†]

The George and Josephine Butler Polymer Research Laboratory, Department of Chemistry, University of Florida, Gainesville, Florida 32611-7200; Department of Chemical and Biomolecular Engineering, University of Pennsylvania, Philadelphia, Pennsylvania 19104-6393; and Department of Materials Science and Engineering, University of Pennsylvania, Philadelphia, Pennsylvania 19104-6272

Received April 10, 2007; Revised Manuscript Received June 29, 2007

ABSTRACT: We report the detailed characterization of strictly linear ethylene-*co*-acrylic acid (EAA) copolymers synthesized via two modes of olefin metathesis polymerization, where control of the polymer microstructure leads to the generation of unique polymer morphologies based on distribution of carboxylic acid moieties along the polymer backbone. Acyclic diene metathesis (ADMET) was used to prepare three high molecular weight, high strength EAA materials bearing pendant carboxylic acid groups along the copolymer backbone precisely placed every 9th, 15th, and 21st carbon, and ring-opening metathesis polymerization (ROMP) was used to create EAA materials of equimolar acid concentrations with irregularly distributed pendant groups along the linear copolymer backbone. Primary structure characterization using FT-IR and NMR techniques are discussed as well as secondary structure analysis via DSC and X-ray scattering. Thermal analysis indicates significant effects of functional group placement on melting temperatures and enthalpies illustrating the importance of ethylene sequence lengths and distributions on polymer crystallization. X-ray scattering reveals broad scattering peaks with evidence of orthorhombic polyethylene-like crystallization in all irregular copolymers except the most highly functionalized, fully amorphous material. The precise carboxylic acid copolymers have X-ray scattering peaks indicative of acid−acid spacing along all-*trans* polyethylene segments of the polymer chain. Only the regularly functionalized EAA copolymer with the lowest acid content is semicrystalline with evidence of orthorhombic polyethylene-like crystallization, while higher concentrations of acids groups lead to amorphous materials. Drawing the semicrystalline ADMET acid copolymer produces an anisotropic morphology, indicating that the acid−acid spacing is parallel to the polyethylene chain axis.

Introduction

The application of ethylene-*co*-acrylic acid (EAA) copolymers to a myriad of end-use applications[1] is possible due to the wide range of material properties available by tuning the interplay between hydrogen bonding and polymer crystallinity.[2] Typically, EAA copolymers are synthesized via standard industrial high-pressure free radical polymerization techniques, and the commercial products come in diverse forms exhibiting varying degrees of microstructural irregularities. While it is this variation in polymer microstructure that allows for a diverse assortment of bulk properties and potential applications, the synthesis of EAA materials with strict control over branching, comonomer distribution, and ethylene sequence length has not been performed.

We report a new family of high molecular weight, high strength, strictly linear EAA copolymers synthesized with specific attention to comonomer incorporation and ethylene sequence length distribution. Prior work on structurally similar materials yielded relatively low molecular weight polymers,[3] where polymerization was limited by the presence of the carboxylic acid group itself, presumably poisoning the metathesis catalyst system. The key synthetic advance described herein has been devising a suitable protection scheme for the acid group allowing for efficient olefin metathesis chemistry to occur in step-growth and chain-growth polymerizations. Consequently, acyclic diene metathesis (ADMET)[4] and ring-opening metathesis polymerization (ROMP)[5] now lead to durable, linear copolymers bearing both precisely spaced and irregularly spaced carboxylic acid moieties along the polymer backbone, as shown in Figure 1.

Approaching EAA synthesis in this manner allows for the production of both precisely functionalized copolymers with monodisperse ethylene run lengths between pendant carboxylic acid groups (ADMET) as well as irregular copolymers with a pseudo-random placement of pendant acid groups and a range of ethylene run lengths (ROMP).[6] Upon hydrogenation of unsaturated olefin metathesis products, fully saturated EAA copolymers were isolated, allowing direct comparison of ethylene sequence length distributions in materials with comparable comonomer ratios to determine the effects of controlled sequence distribution on bulk copolymer morphology. Primary structural analysis using FT-IR and NMR techniques is discussed, illustrating the control allowed over copolymer synthesis applying the metathesis−hydrogenation route. Detailed calorimetry and X-ray scattering data are presented to illustrate the morphology differences between regular and irregular distributions of functional groups.

Experimental Section

Materials. All chemicals were purchased from Aldrich and used as received, unless otherwise specified. Cyclooctene was dried over

* Corresponding authors. E-mail: wagener@chem.ufl.edu, winey@seas.upenn.edu.
[†] University of Florida.
[‡] Department of Chemical and Biomolecular Engineering, University of Pennsylvania.
[§] Department of Materials Science and Engineering, University of Pennsylvania.

10.1021/ma070841r CCC: $37.00
Published on Web 08/09/2007

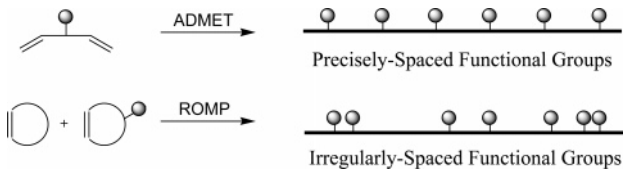

Figure 1. Copolymer synthesis using olefin metathesis−hydrogenation strategy.

CaH_2 and freshly distilled prior to use. First generation Grubbs' catalyst was a gift from Materia, Inc., and was used as received. Preparation of 2-(4-cyclooctenyl)acetic acid,[7] 2-(4-pentenyl)-6-hepteneoic acid, 2-(7-octenyl)-9-deceneoic acid, and 2-(10-undecenyl)-12-trideceneoic acid[8] was performed as previously reported.

Instrumentation and Analysis. All ^{1}H NMR (300 MHz) and ^{13}C NMR (75 MHz) spectra were recorded on a Varian Associates Mercury 300 spectrometer. Chemical shifts for ^{1}H and ^{13}C NMR were referenced to residual signals from dioxane-d_8 (^{1}H: $\delta = 3.53$ ppm and ^{13}C: $\delta = 39.50$ ppm), THF-d_8 (^{1}H: $\delta = 3.58$ ppm and ^{13}C: $\delta = 25.4$ ppm), or $CDCl_3$ (^{1}H: $\delta = 7.27$ ppm and ^{13}C: $\delta = 77.23$ ppm) with 0.03% v/v TMS as an internal reference. Thin layer chromatography (TLC) was performed on EMD silica gel-coated (250 μm thickness) glass plates. Developed TLC plates were stained with iodine absorbed on silica to produce a visible signature. Reaction conversions and relative purity of crude products were monitored by TLC chromatography and ^{1}H NMR. Fourier transform infrared (FT-IR) measurements were conducted on polymer films cast from chloroform onto KBr plates using a Bruker Vector 22 infrared spectrophotometer.

Differential scanning calorimetry (DSC) was performed using a TA Instruments Q1000 or a TA Instruments 2920 at a heating rate of 10 °C/min under nitrogen or helium purge. Calibrations were made using indium and freshly distilled *n*-octane as the standards for peak temperature transitions and indium for the enthalpy standard. All samples were prepared in hermetically sealed pans (3−7 mg/sample) and were run using an empty pan as a reference. Thermogravimetric analysis (TGA) was performed on a TA Q500 using the dynamic high-resolution analysis mode.

Gel permeation chromatography (GPC) was performed using a Waters Associates GPCV2000 liquid chromatography system with its internal differential refractive index detector (DRI) at 40 °C using two Waters Styragel HR-5E columns (10 μm PD, 7.8 mm i.d., 300 mm length) with HPLC grade THF as the mobile phase at a flow rate of 1.0 mL/min. Injections were made at 0.05−0.07% w/v sample concentration using a 220.5 μL injection volume. Retention times were calibrated against narrow molecular weight polystyrene standards (Polymer Laboratories; Amherst, MA). All standards were selected to include M_p or M_w values well beyond the expected polymer's range.

The X-ray scattering apparatus consists of a Nonius FR591 rotating anode generator operated at 40 kV and 85 mA, mirror−monochromator focusing optics, an evacuated flight path, and a Brüker HiSTAR two-dimensional detector. Data were acquired for 1 h at a sample−detector distance of 11 or 124 cm. 2D data reduction, analysis, and curve fitting were performed using Datasqueeze software.[9]

Sample Preparation for DSC and X-ray Analysis. The fast cooled samples were melt-pressed in a Carver 4122 hot press at 150 °C and then subjected to rapid cooling in the press by flowing tap water (∼8 °C/min). The slow cooled samples were melt-pressed, the heaters in the press were turned off, and the press and sample were slowly cooled to room temperature in (∼0.5 °C/min). The drawn samples are fast cooled samples that were reheated by a hot air gun, elongated while soft, and cooled rapidly in air (∼200 °C/min).

Monomer Synthesis. General Procedure for Acid Protection. A solution of 2-(4-pentenyl)-6-hepteneoic acid (1 equiv) in diethyl ether (20 mL) was slowly added via Pasteur pipet to a cooled (0 °C) solution of ethyl vinyl ether (excess, usually >4 equiv) and phosphoric acid (cat., 1 drop from capillary pipet) in diethyl ether (10 mL). The solution was stirred cold for 30 min under argon and then warmed to room temperature for 3 days. Basic alumina (∼1 g) was added to the reaction mixture and stirred for 5 min. After filtration and solvent removal, **1** was isolated as 7.3 g (99.0% yield) of colorless oil with no further purification required.

1-Ethoxyethyl-2-(pent-4-enyl)hept-6-enoate (1). 98.2% yield. ^{1}H NMR ($CDCl_3$): δ (ppm) 1.22 (t, 3H) 1.30−1.55 (br, 9H), 1.62 (m, 2H), 2.05 (q, 4H), 2.36 (m, 1H), 3.53 (d, 1H), 3.71 (m, 1H), 4.97 (m, 4H), 5.82 (m, 2H), 5.94 (q, 1H). ^{13}C NMR ($CDCl_3$): δ (ppm) 15.24, 21.14, 26.86, 26.89, 31.91, 32.10, 33.76, 45.98, 64.77, 96.33, 114.92, 138.56, 176.17.

1-Ethoxyethyl-2-(oct-7-enyl)dec-9-enoate (2). 99.1% yield. ^{1}H NMR ($CDCl_3$): δ (ppm) 1.16−1.53 (br, 24H), 1.61 (m, 2H), 2.04 (q, 4H), 2.34 (m, 1H), 3.53 (m, 1H), 3.71 (m, 1H), 4.97 (m, 4H), 5.81 (m, 2H), 5.95 (q, 1H). ^{13}C NMR ($CDCl_3$): δ (ppm) 15.24, 21.13, 27.59, 27.65, 29.03, 29.15, 29.58, 32.52, 32.71, 33.94, 46.30, 64.72, 96.22, 114.41, 139.27, 176.42.

1-Ethoxyethyl-2-(undec-10-enyl)tridec-12-enoate (3). 98.4% yield. ^{1}H NMR ($CDCl_3$): δ (ppm) 1.16−1.53 (br, 36H), 1.60 (m, 2H), 2.04 (q, 4H), 2.33 (m, 1H), 3.54 (m, 1H), 3.71 (m, 1H), 4.97 (m, 4H), 5.81 (m, 2H), 5.95 (q, 1H). ^{13}C NMR ($CDCl_3$): δ (ppm) 15.24, 21.13, 27.59, 27.65, 29.03, 29.15, 29.58, 32.52, 32.71, 33.94, 46.30, 64.72, 96.22, 114.41, 139.27, 176.42.

1-Ethoxyethyl-2-(cyclo-4-octenyl)acetate (4). Prepared from 2-(4-cyclooctenyl)acetic acid. ^{1}H NMR ($CDCl_3$): δ (ppm) 1.19 (t, 3H), 1.40 (d, 3H), 1.51−1.79 (br, 3H), 1.98−2.25 (br, 4H), 2.38 (m, 1H), 2.47 (m, 1H), 3.52 (m, 1H), 3.69 (m, 1H), 5.66 (m, 2H), 5.92 (q, 1H). ^{13}C NMR ($CDCl_3$): δ (ppm) 15.26, 21.02, 24.32, 26.08, 26.11, 28.02, 29.51, 29.63, 31.77, 31.91, 43.86, 64.72, 64.78, 96.18, 129.71, 129.75, 130.74, 130.81, 177.55, 177.57.

General Procedure for ADMET Polymerization. 1-Ethoxyethyl-2-(pent-4-enyl)hept-6-enoate (**1**, 1 g) was added to a 50 mL round-bottomed flask equipped with a magnetic stir bar and degassed by stirring under high vacuum for 1 h. Grubbs' first-generation catalyst (400:1 monomer:catalyst) was added to the flask, and high vacuum (10^{-4} Torr) was applied slowly over 1 h, and then the temperature was raised to 50 °C for 72 h. Upon cooling the room temperature, ethyl vinyl ether (∼10 drops) in toluene (50 mL) was added to the polymerization flask and stirred until all solids dissolved. Precipitation of the crude solution into acidic MeOH (500 mL, 0.5 M HCl) and subsequent filtration followed by vacuum drying afforded 987 mg of unsaturated polymer as brown tacky solid.

Polymerization of 1 for 22 mol % AA (5). ^{1}H NMR ($CDCl_3$): δ (ppm) 1.16−1.51 (br, 12H), 1.60 (m, 2H), 1.97 (q, 4H), 2.33 (m, 1H), 3.53 (m, 1H), 3.70 (m, 1H), 5.35 (m, 2H), 5.94 (q, 1H). ^{13}C NMR ($CDCl_3$): δ (ppm) 15.27, 21.15, 27.31, 27.62, 32.09, 32.29, 32.65, 46.06, 64.73, 96.26, 129.83, 130.32, 176.21; FT-IR: (cm^{-1}) 2978, 2926, 2854, 1733, 1704, 1464, 1376, 1124, 1039, 948, 965, 849, 723.

Polymerization of 2 for 13 mol % AA (6). ^{1}H NMR ($CDCl_3$): δ (ppm) 1.16−1.51 (br, 24H), 1.60 (m, 2H), 1.95 (q, 4H), 2.32 (m, 1H), 3.53 (m, 1H), 3.71 (m, 1H), 5.35 (m, 2H), 5.95 (q, 1H). ^{13}C NMR ($CDCl_3$): δ (ppm) 15.25, 21.14, 27.41, 27.66, 27.72, 29.27, 29.40, 29.64, 29.79, 29.91, 32.60, 32.79, 46.36, 64.72, 96.20, 130.02, 130.49, 176.46. FT-IR (cm^{-1}): 2977, 2926, 2852, 1732, 1704, 1463, 1376, 1124, 1037, 948, 965, 852, 721.

Polymerization of 3 for 9.5 mol % AA (7). ^{1}H NMR ($CDCl_3$): δ (ppm) 1.30−1.51 (br, 36H), 1.60 (m, 2H), 1.96 (q, 4H), 2.32 (m, 1H), 3.53 (m, 1H), 3.71 (m, 1H), 5.38 (m, 2H), 5.95 (q, 1H). ^{13}C NMR ($CDCl_3$): δ (ppm) 15.26, 21.15, 27.45, 27.70, 27.75, 29.42, 29.55, 29.90, 30.00, 32.84, 46.37, 64.71, 96.19, 130.02, 130.08, 130.54, 176.46. FT-IR (cm^{-1}): 2978, 2925, 2854, 1732, 1705, 1463, 1378, 1124, 1037, 948, 966, 852, 722.

General Conditions for ROMP Copolymerization. Cyclooctene (0.55 g, 5.0 mmol) and **4** (9.00 g, 39.7 mmol) were added toluene (30 mL) in a 200 mL round-bottomed flask under nitrogen purge. The reaction mixture was heated to 50 °C, and a solution of Grubbs' first-generation catalyst (53 mg, 6.4 μmol, 1000:1 monomer:catalyst) in dichloromethane (0.5 mL) was added to the magnetically stirred reaction mixture. After 3−6 h, the polymerization mixture was quenched by addition of ethyl vinyl ether (∼10 drops) and

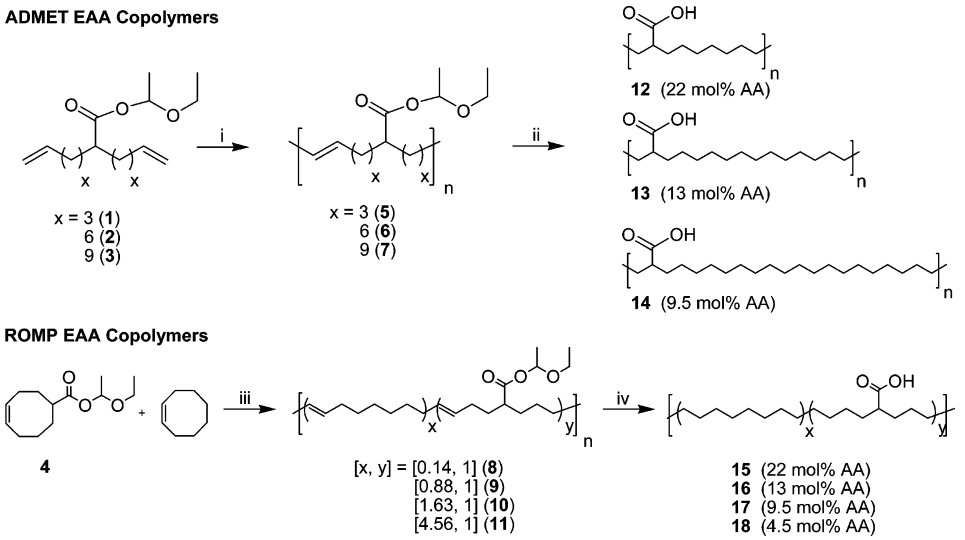

Figure 2. EAA copolymer synthesis: (i) first-generation Grubbs' catalyst, vacuum (10^{-3} mmHg); (ii) H_2 (400 psi), $RhCl(PPh_3)_3$, toluene, 1-butanol, 60 °C; (iii) first-generation Grubbs catalyst, toluene, 60 °C; (ii) H_2 (400 psi), $RhCl(PPh_3)_3$, toluene, 1-butanol, 60−100 °C.

allowed to stir for 5 min. Upon precipitation of crude solution into acidic (1 M HCl) methanol, the unsaturated polymer product was isolated as a mildly adhesive solid. No further purification of unsaturated prepolymers was necessary.

For 22 mol % AA (8). ^{13}C NMR ($CDCl_3$): δ (ppm) 15.27, 21.16, 27.31, 27.61, 32.10, 32.30, 32.66, 46.08, 64.73, 96.26, 129.84, 130.33, 176.21. FT-IR (cm^{-1}): 2978, 2926, 2854, 1733, 1704, 1464, 1375, 1124, 1039, 949, 966, 849, 723.

For 13 mol % AA (9). ^{13}C NMR ($CDCl_3$): δ (ppm) 15.27, 21.16, 27.30, 27.61, 32.10, 32.30, 32.66, 46.10, 64.73, 96.26, 129.85, 130.33, 176.21. FT-IR (cm^{-1}): 2980, 2926, 2853, 1733, 1704, 1464, 1376, 1122, 1041, 948, 966, 849, 723.

For 9.5 mol % AA (10). ^{13}C NMR ($CDCl_3$): δ (ppm) 15.26, 21.16, 27.31, 27.61, 32.10, 32.30, 32.66, 46.08, 64.73, 96.27, 129.84, 130.33, 176.21. FT-IR (cm^{-1}): 2978, 2927, 2854, 1733, 1704, 1464, 1375, 1125, 1039, 948, 965, 849, 721.

For 4.5 mol % AA (11). ^{13}C NMR ($CDCl_3$): δ (ppm) 15.27, 21.15, 27.31, 27.61, 32.11, 32.30, 32.66, 46.08, 64.73, 96.25, 129.84, 130.31, 176.21. FT-IR (cm^{-1}): 2978, 2926, 2855, 1733, 1705, 1464, 1376, 1124, 1039, 948, 965, 849, 722.

Hydrogenation of Unsaturated ADMET and ROMP Products. General Conditions for Parr Bomb Hydrogenation. A solution of **6** (1.0 g, 4.45 mol olefin) was dissolved in a toluene (100 mL) and 1-butanol (50 mL) mixture and then degassed by bubbling a nitrogen purge through the stirred solution for 30 min. Solid Wilkinson's catalyst (3.7 mg, 4 μmol) [$RhCl(PPh_3)_3$] was added to the solution, and the glass sleeve was sealed in a Parr reactor equipped with a temperature probe, pressure gauge, and a paddle wheel stirrer. The reactor was filled to 400 psi hydrogen gas and purge three times while stirring, filled to 400 psi hydrogen, and heated to 80 °C for 48 h. Upon cooling to room temperature and safely releasing pressure using a vent valve, the crude solution was precipitated into methanol, filtered, and dried, affording 994 mg (99% yield) of saturated EAA copolymer.

Hydrogenation of 5 (12). ^1H NMR (dioxane-d_8): δ (ppm) 1.19−1.65 (br, 16H), 2.24 (m, 1H). ^{13}C NMR (dioxane-d_8): δ (ppm) 28.21, 30.21, 30.27, 30.36, 33.14, 45.93, 177.41. FT-IR (ν, cm^{-1}): 2921, 2852, 1704, 1461, 1418, 1287, 1235, 931, 721.

Hydrogenation of 6 (13). ^1H NMR (dioxane-d_8): δ (ppm) 1.20−1.65 (br, 28H), 2.24 (m, 1H). ^{13}C NMR (dioxane-d_8): δ (ppm) 28.21, 30.28, 30.38, 30.43, 33.10, 45.89, 177.43. FT-IR (ν, cm^{-1}): 2921, 2852, 1704, 1461, 1417, 1288, 1234, 930, 721.

Hydrogenation of 7 (14). ^1H NMR (dioxane-d_8): δ (ppm) 1.07−1.65 (br, 40H), 2.25 (m, 1H). ^{13}C NMR (THF-d_8): δ (ppm) 28.60, 30.69, 30.85, 33.57, 46.32, 177.29. FT-IR (ν, cm^{-1}): 2920, 2851, 1704, 1461, 1419, 1288, 1235, 933, 723

Parr Bomb Hydrogenation Procedure. Same procedure as described previously for ADMET EAA materials, but these reactions were run at temperatures over 100 °C to ensure reaction product solubility.

Hydrogenation of 8 (15). FT-IR (ν, cm^{-1}): 2920, 2850, 1704, 1460, 719.

Hydrogenation of 9 (16). FT-IR (ν, cm^{-1}): 2919, 2851, 1705, 1466, 721.

Hydrogenation of 10 (17). FT-IR (ν, cm^{-1}): 2920, 2850, 1704, 1469, 715.

Hydrogenation of 11 (18). FT-IR (ν, cm^{-1}): 2920, 2850, 1705, 1469, 715.

Results and Discussion

The synthesis of linear EAA copolymers required the preparation of unsaturated monomers for both the ADMET and ROMP reactions. Symmetrical acid bearing dienes and an acid-functionalized cyclooctene were prepared by previously reported methods.[7,8] Prior to polymerization, acid monomers were protected with a unique hemiacetal ester moiety[10] to prevent metathesis catalyst decomposition and allow for conversion back to the free carboxylic acid either by thermal deprotection or during the subsequent polymer hydrogenation reaction. This protection scheme is key to the formation of high molecular weight, high strength materials where preliminary mechanical measurements reveal tensile strengths in excess of 4500 psi and elongations to break in excess of 450% for a sample of melt-cast polymer **14**.

Metathesis polymerizations for all protected monomers were performed as detailed in Figure 2. ADMET polymerization of protected acids proceeded normally with little if any effect from the hemiacetal ester on the reaction, but some cleavage of protecting groups was observed (FT-IR) during ROMP reactions when run longer than 3 h, although no effect on copolymer structure or polydispersity was observed. Protected, unsaturated polymers were isolated at typical molecular weights for both methods, and characterization data for both unsaturated metathesis products and saturated EAA copolymers are compiled in Table 2. As mentioned previously, hydrogenation and deprotection of polymers were performed using Wilkinson's catalyst under hydrogen pressure in a Parr reactor. A binary solvent mixture of toluene and 1-butanol was employed to ensure both starting material and product solubility while also having the added effect of reducing reaction times compared to a single solvent.

Table 1. EAA Copolymer Characterization Data

		GPC data[b]		
polymer	mol % acrylic acid[a]	M_n	M_w	PDI
12	22	25.1	40.8	1.62
13	13	31.8	59.1	1.86
14	9.5	37.7	65.2	1.73
15	22	85.0	106.2	1.25
16[c]	13	80.5	111.1	1.38
17[c]	9.5	85.4	163.9	1.41
18[c]	4.5	93.6	128.2	1.37

[a] Calculated from theoretical repeat unit, confirmed by ^{1}H NMR. [b] Reported in kg/mol and performed in THF at 40 °C with calibration against PS standards. [c] Insoluble copolymer; GPC data from protected, unsaturated parent material.

Table 2. Thermal Analysis of Linear EAA Copolymers

		DSC data[b]			
	mol % acrylic acid[a]	T_g (°C)	ΔC_p (J/(g °C))	T_m (°C)	ΔH_m (J/g)
ADMET copolymers					
12	22	22	0.4		
13	13	−4	0.5		
14	9.5			45	42
ROMP copolymers					
15	22	−22	0.3		
16	13			74	51
17	9.5			85	75
18	4.5			98	78

[a] Calculated from theoretical repeat unit, confirmed by ^{1}H NMR. [b] 10 °C/min scan rate; values calculated from second scan data.

Characterization data for fully saturated materials are reported in Table 1, but the limited solubility of a few of these materials precludes them from many forms of solution-based analysis including NMR or GPC. In these cases, molecular weight values and acid functionalization levels from the parent protected, unsaturated polymers were reported as values for their saturated analogues. This method was deemed suitable as soluble, saturated EAA ADMET copolymers showed absolutely no molecular weight degradation or observable side reactions applying aforementioned hydrogenation conditions. In all cases, GPC analysis of even the soluble EAA copolymers was difficult due to hydrogen-bonding-induced polymer aggregation.

Primary structure analysis by ^{1}H NMR reveals the pristine polymer microstructures in sequenced ADMET materials produced by clean metathesis and hydrogenation chemistries. While the proton spectrum is simple, it displays the structural purity of the ADMET materials and allows for determination of molar ratios of ethylene and acrylic acid by integration of the indicated peak in the inset of Figure 3b. For pseudo-random materials only soluble in binary or boiling solvents (**16**−**18**), the soluble, unsaturated parent polymers were analyzed in this fashion to determine molar concentration of ester functionality and confirm successful ROMP copolymerization.

For the carbon spectrum in Figure 3b, resonances for the carbonyl (A = 177.3 ppm), α (B = 46.3 ppm), β (C = 33.6 ppm), and γ (D = 28.6 ppm) carbons can be resolved with remaining methylene carbons overlapping near 30.7 ppm. Here again, the microstructural control afforded with ADMET polymerization is displayed in the symmetrical signal pattern of C and D and the limited number of resonances observed between 20 and 35 ppm.

FT-IR absorbance data for solution cast **14** are displayed in Figure 3c. The presence of a single absorbance at 1705 cm^{-1} not only confirms quantitative deprotection of the parent ester polymer but also indicates the prevalent dimerization of carboxylic acid groups throughout the material with no free acids

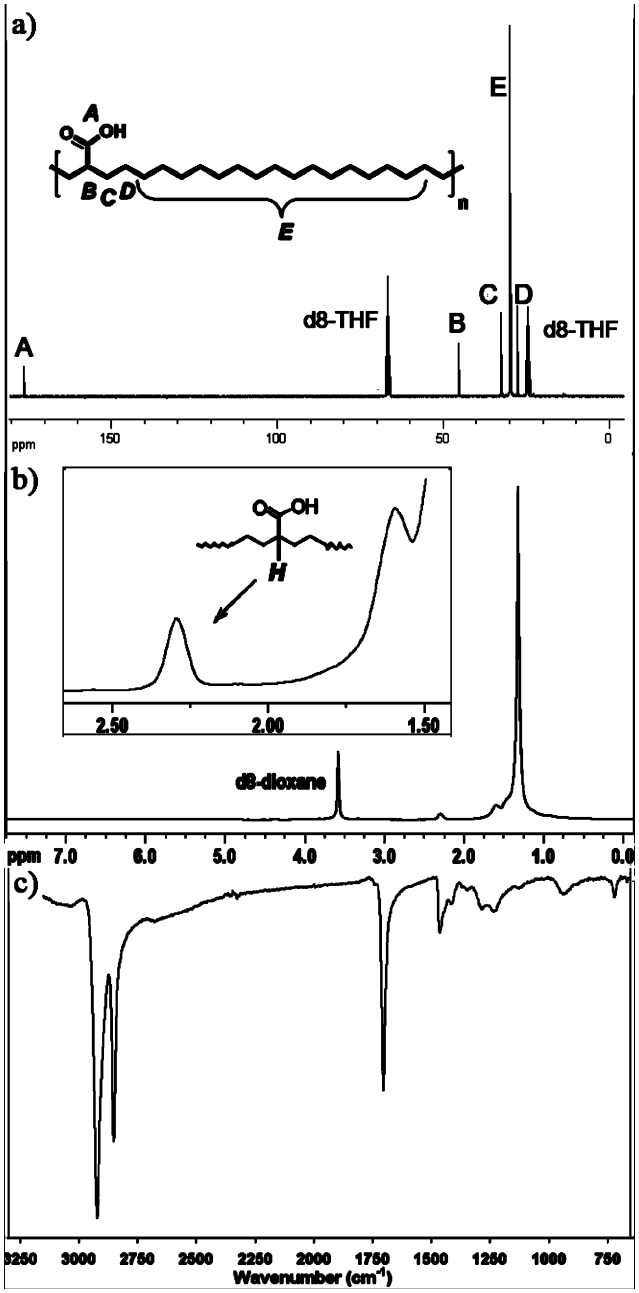

Figure 3. Structural analysis for EAA copolymer **14**: (a) ^{13}C NMR, (b) ^{1}H NMR, and (c) FT-IR.

(1750 cm^{-1}) observed for any EAA copolymers in this study.[2] The propensity for carboxylic acids to self-associate in this manner creates dynamic physical cross-links in EAA materials regardless of acid content or sequence length distribution. This feature of EAA copolymer morphology is not unique to ADMET and ROMP prepared materials, and it is commonly observed for commercial EAA copolymers as one of the strongest associative forces observed in ethylene copolymers, thereby altering polymer chain packing and crystallization.[2] Another feature in the FT-IR spectra critical to chain packing and bulk polymer morphology is the peak appearing at 720 cm^{-1} corresponding to the methylene rocking vibrations, usually seen in orthorhombic crystal packing of the polymer backbone.[11] Although the absorbance maximum indicates crystalline order, the breadth of this peak indicates some level of disorder within the material also accounting for the methylene segments portions trapped in amorphous regions of the material. This structural

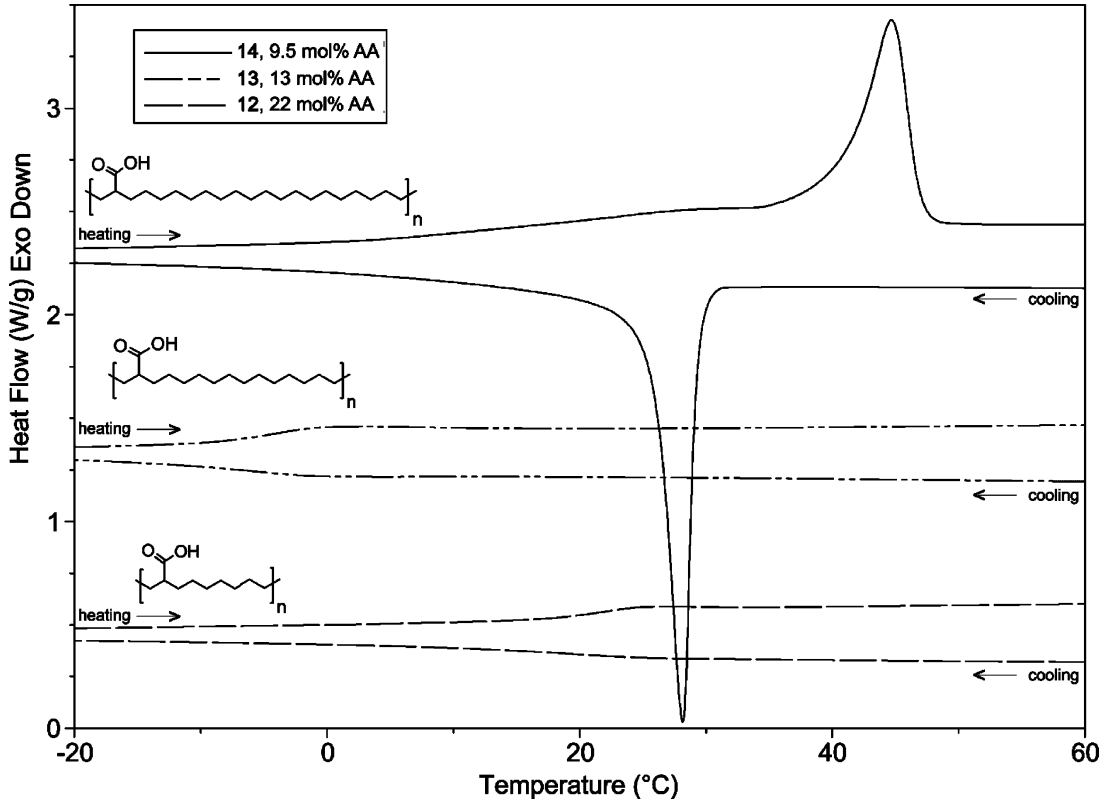

Figure 4. DSC of ADMET EAA copolymers (arbitrary vertical offsets for clarity).

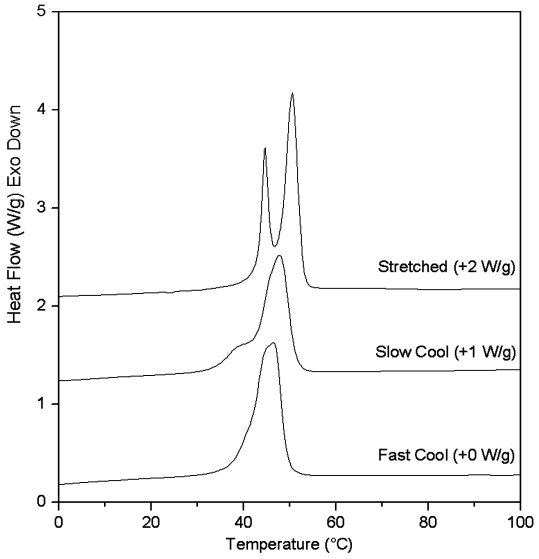

Figure 5. DSC of heat-treated films of polymer **14** (arbitrary vertical offsets for clarity).

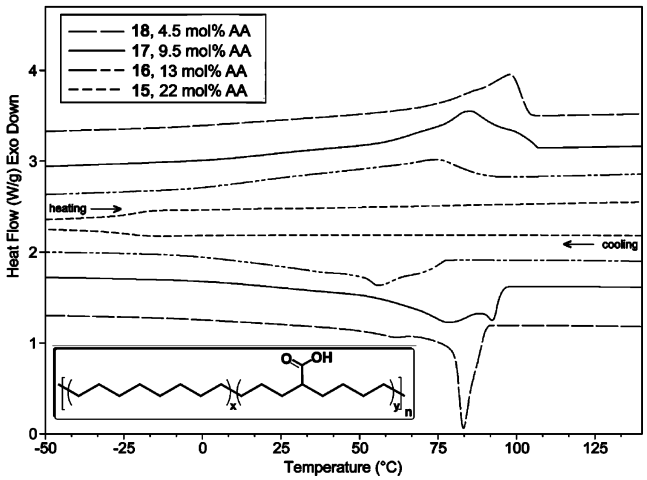

Figure 6. DSC of ROMP EAA copolymers **15**−**18** using arbitrary vertical offsets for clarity.

analysis is supported by X-ray scattering data discussed later in the paper.

Differential scanning calorimetry (DSC) was performed on linear EAA copolymers, and data and thermal profiles for all materials are presented in Table 2 and Figures 4−6. It is clear from this data that the distribution of functional groups and/or ethylene sequence lengths within a polymeric material has drastic effects on polymer morphology and thermal behavior. For ADMET EAA copolymers (Figure 4), the thermal data are typical for most sequenced materials, where decreasing the pendant branch frequency (increasing the molar concentration on acrylic acid) yields less crystalline materials until, at some point, completely amorphous copolymers result due to increased steric congestion along the polymer backbone.[12] In the case of acid-functionalized polymers, only **14** displays melting behavior as indicated by a large endothermic transition at 45 °C (ΔH_m = 42 J/g), while **12** and **13** display fully amorphous character exhibiting clear glass transition temperatures at 22 °C (ΔC_p = 0.4 J/(g °C)) and −4 °C (ΔC_p = 0.5 J/(g °C)), respectively. The relationship between glass transition values and chain flexibility for polymers **12** and **13** becomes clear as molar concentration of dimerized acid groups (physical cross-links) is considered. The less cross-linked structure of **13** gives way to greater chain flexibility and lower T_g, while polymer **12** exists in a less mobile state due to the more extensive hydrogen bonding that inhibits polymer chain motion. The boundary between amorphous and semicrystalline materials in this family of copolymers resides at a longer ethylene sequences (lower degree of functionalization) than most ADMET copolymer series.[12] This observation further confirms that secondary

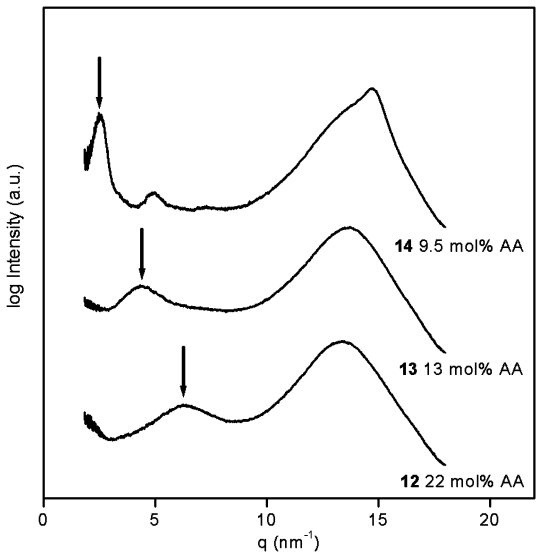

Figure 7. X-ray scattering of precise carboxylic acid copolymers **14**, **13**, and **12**; only **14** (9.5 mol % AA) exhibits a crystalline peak near the (110) crystalline peak of orthorhombic polyethylene at 14.8 nm^{-1}. The arrows point to new peaks in the X-ray pattern, which are consistent with the distance between periodically placed acid groups.

interactions, in this case acid−acid dimerization, impede polymer backbone nucleation and ultimate crystallization.

Cooling rate and mechanical stretching alter the thermal transitions observed in these ADMET copolymers. The fast cooled sample of polymer **14** has a melting peak at 47 °C, while the slow cooled sample has a comparable melting point at 48 °C and a lower onset temperature (Figure 5). Slow cooling apparently allows the growth of secondary crystallites with lower melting temperatures. Interestingly, the drawn sample melts at two distinct temperatures, 44 and 50 °C. This double melting peak suggests the presence of primary and secondary crystallites in the drawn material. The DSC data from the samples of polymer **14** was also used to *estimate* the degree of crystallization based on the polyethylene enthalpy of melting (277.1 J/g):[13] fast cooled ∼23%, slow cooled ∼20%, and drawn ∼25%.

Analysis of ROMP materials follows more closely to that of typical ethylene copolymers where a consistent increase in peak melting temperature and heat of fusion is linked with a decrease in comonomer content (Table 2, Figure 6). Although the limited variability of sequence lengths created during ROMP polymerization[6] seem to have little effect on polymer crystallinity up to 13 mol % acrylic acid (**16**), the 22 mol % acrylic acid (**15**) copolymer is completely amorphous on first and second heating scans while industrial materials of similar composition maintain their semicrystallinity at this level of functionalization.[14] The lack of long, uninterrupted ethylene sequences and presence of fairly well distributed acid units in **15** created during the ROMP process is the result of having a minimum run length corresponding to a ring-opened cyclooctene.[6] This and the presence of dimerized acid groups creates a dense hydrogen-bond matrix within this material impeding chain motion and preventing crystallization.

Secondary structure analysis of X-ray scattering data provides valuable insights into the morphology of both the crystalline and amorphous materials. For EAA copolymers in this study, the large differences in thermal behavior presented in the previous section can be correlated to changes in the polymer morphology arising from the ethylene sequence length distribution and acid−acid dimer location within the copolymers.

In all of the precise carboxylic acid copolymers prepared via ADMET, fast cooled samples exhibit an amorphous scattering peak at ∼13.5 nm^{-1} (Figure 7), indicating the presence of randomly oriented polymer backbones. Fast-cooled **14** also shows a reflection at 14.8 nm^{-1} corresponding to the (110) peak that is typical of orthorhombic polyethylene and directly related to the melting event observed in DSC experiments. All precise EAA materials display peaks at lower *q*, as indicated by the arrows in Figure 7. The relatively sharp peaks at 2.48, 4.81, and 7.55 nm^{-1} in sample **14** correspond to multiple orders of diffraction from a spacing of 2.53 nm. This experimental spacing is comparable to the distance between acid groups in **14** when the polyethylene chain conformation is all-*trans*, which is calculated to be 2.66 nm.[15] For the more highly functionalized, precise EAA copolymers, this acid−acid scattering peak shifts to higher *q*, as expected, as the acid content increases in samples **13** and **12**. With higher acid concentration and regular sequence distribution along the polymer chain, the acid−acid distances

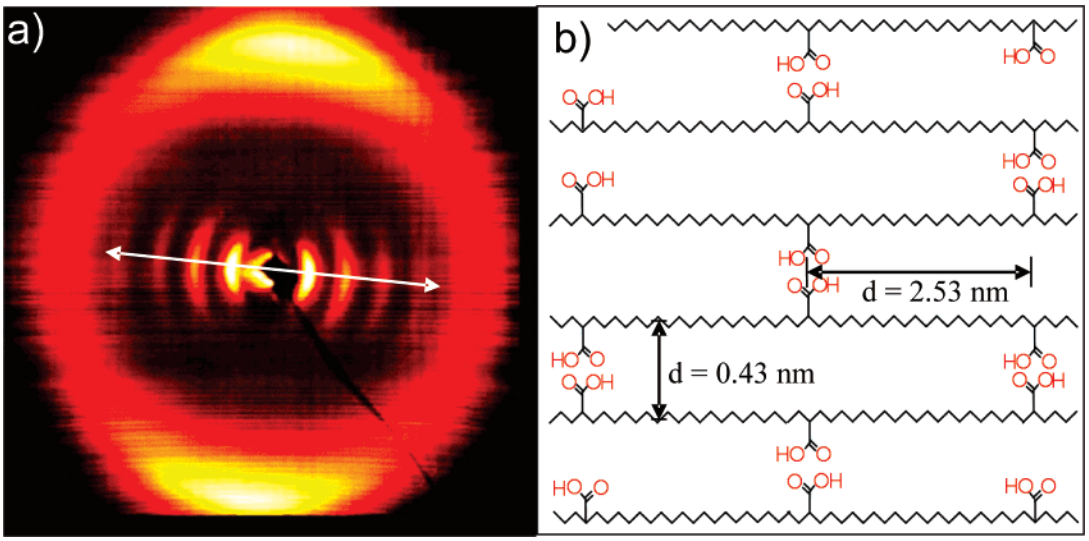

Figure 8. (a) X-ray scattering pattern of a sample made from polymer **14** stretched along the arrow direction. High-intensity arcs at 14.8 nm^{-1} are similar to the (110) reflection of orthorhombic polyethylene. Multiple reflections of 2.48 nm^{-1} indicate a layered structure with a 2.53 nm spacing oriented perpendicular to the polyethylene backbone. (b) A schematic of the ethylene chain segments and acid groups arranged within a crystalline domain. For simplicity, the schematic only shows H-bonds formed between polymers in this plane, although H-bonds can form with acid groups from polymers above and below those drawn.

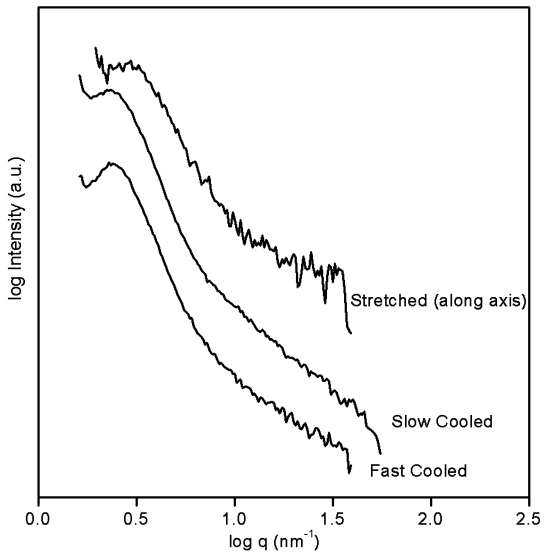

Figure 9. Small-angle X-ray data of the **14** heat-treated DSC samples shows the lamellae−lamellae spacing.

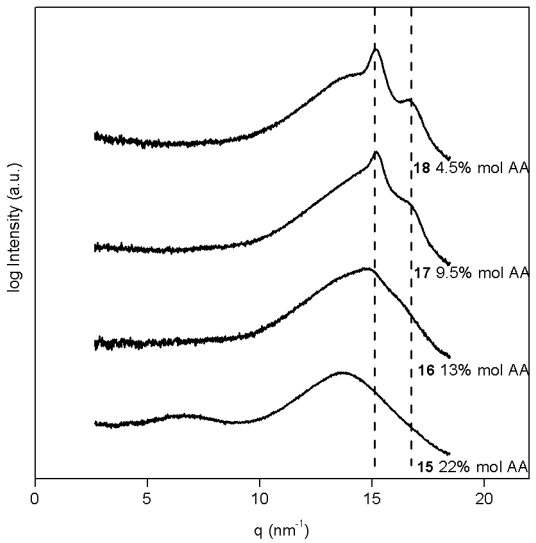

Figure 10. X-ray scattering of statistical copolymers **15**−**18**. The (110) and (200) peaks of polyethylene orthorhombic unit cell are detected in **18**, **17**, and **16** but are not detected in **15** (22 mol % AA). The most highly functionalized copolymer, **15**, also has an extra peak at 6.6 nm^{-1} which suggests a pseudoperiodic placement of the acids along the main-chain backbone.

become shorter in the all-*trans* conformations, leading to scattering peaks at higher *q*. The breadth of these scattering peaks tends to increase relative to peaks for **14** and is due to the less ordered nature of **12** and **13**.

One well-known method of producing anisotropy in polyethylene materials is drawing. Analyzing a drawn sample of the semicrystalline **14**, a 90° orientation between the low-angle acid−acid peak and the polyethylene (110) peak is displayed in Figure 8a. (Note, this drawing method failed to induce anisotropy in samples 12 and 13.) Specifically, drawing **14** aligns the polymer backbone along the draw direction and orients the planes containing the acid groups perpendicular to the draw direction. Figure 8b shows a two-dimensional schematic of the polyethylene chain segments and acid groups arranged within a crystalline domain consistent with the scattering data. Because of the atacticity of this material, the acid groups will form H-bonds with different neighboring polyethylene chains within a crystal. For simplicity, the schematic shows H-bonds between polymers in the plane; acid groups also form H-bonds with acid groups from polymers above and below the crystal plane shown. The dimerization of the carboxylic acids constrains these groups to a planar region within the orthorhombic PE crystal. Note that all the carboxylic acid groups are paired as determined by FT-IR. In contrast, others have reported that precisely placed −Cl, −Br, and $-CH_3$ groups in similarly prepared materials transforms the orthorhombic structure to a triclinic structure.[16,17] The acid-layered structure we report here is the combined result of pairwise interactions of dimerized acid units along with the precise distribution of these groups along the polymer backbone.

The small-angle X-ray data from **14** samples in Figure 9 indicate that the lamellae−lamellae periodicities are similar for the three processing method discussed in Figure 5. The lamellae−lamellae scattering peaks at 0.378, 0.390, and 0.491 nm^{-1} for the slow-cooled, fast-cooled, and drawn **14** samples, respectively, correspond to spacings of 16.6, 16.1, and 12.8 nm according to Bragg's law. Using these periodicities, the estimated percent crystallinity (∼20−25%), and the acid−acid spacing of 2.53 in **14**, we estimate that each lamellae is ∼2.6−4.2 nm thick and contains 2−3 acid-rich layers. This number of acid-rich layers serves as a lower limit because the percent crystallinity might be higher due to a depletion of the amorphous phase between the stacked lamellae and/or a lower enthalpy of melting in these ADMET copolymers relative to PE. In contrast, a linear polyethylene (without acid groups), routinely forms semicrystalline morphologies with thicker lamellae, 6−20 nm thick.[18] These structural characterizations combine to indicate that the extent of a PE crystal along the *c*-axis is reduced by the regular placement of carboxylic acid groups. As the acrylic acid concentration increases from 9.5 to 22 mol %, both DSC and scattering data indicate the loss of crystallinity, while the acid−acid spacing persists and decreases in dimension (Figure 7). The highest acid content copolymer, **12**, has a mere eight carbons between acid groups, so that even if lamellae form, they might be too thin or too defective to give a signal in either DSC or X-ray scattering.

Similar characterization of copolymers with irregular placement of carboxylic acids detects the (110) and (200) peaks of orthorhombic polyethylene in all the ROMP copolymers except **15** (Figure 10). Here again, the presence of the acid groups does not transform the orthorhombic unit cell, but even a modest amount of acid (**18**, **17**, and **16**) significantly reduces the apparent degree of crystallinity. These results directly correlate with DSC data as **15** is the only amorphous, ROMP copolymer in this study. For semicrystalline, irregular EAA copolymers, the acid−acid peak is absent at lower angles because the random placement of the acid groups accommodates the H-bonding acid dimerization without producing periodic acid-rich layers above, below, and within the lamellae. Interestingly, the highest acid content, irregular copolymer, **15**, was prepared with an 8 to 1 ratio of 2-(4-cyclooctenyl)acetic acid to 4-cyclooctene creating a pseudoperiodic acid placement along the linear polymer. This pseudoperiodic sequence distribution is sufficient to give a weak peak at ∼6 nm^{-1} (Figure 10) from the acid−acid spacing within this copolymer, and the peak position is comparable to that of sample **12** (Figure 7), which also has 22 mol % acid.

Conclusion

We have described a family of high molecular weight, strictly linear EAA copolymers prepared by applying two modes of olefin metathesis polymerization affording precise and irregular ethylene sequence length distributions. Thermal analysis and X-ray data indicate significant morphology differences between

the two groups of copolymers based entirely on functional group distribution along the polymer backbone. The irregularly functionalized EAA copolymers prepared by ROMP have typical morphologies by X-ray analysis (though the highest acid content copolymer exhibits an acid−acid spacing) and indicate an increase in overall polymer crystallinity as the level of acrylic acid decreases, similar to many examples of commercial materials. For ADMET materials having monodisperse ethylene sequence lengths, the steric congestion of hydrogen-bonded acid dimers impedes polymer chain nucleation and crystallization for highly functionalized material although these materials exhibit a characteristic length of acid−acid spacing. Furthermore, **14** (9.5 mol % AA) has a semicrystalline behavior where the orthorhombic crystalline lattice of EAA copolymers is not significantly distorted to accommodate the dimerized acid units and the acid-rich layers are perpendicular to the polymer chains. These new morphologies organize the functional groups into larger structures that could have profound effects on properties.

Acknowledgment. The authors thank the Florida Space Grant Consortium (NASA-FSGC: NASA-NGT5-40107) and the National Science Foundation (NSF: 0314110, DMR0549116, DAAD19-03-1-0130) for financial support as well as the Army Research Office (ARO: DAAD19-03-1-0083) for its support of catalyst development. We also thank Dr. Stephen "Ed" Lehman for synthetic advice and Kathleen Opper for tensile measurements.

References and Notes

(1) http://www2.dupont.com/Nucrel/en_US/, as of May 28, 2007.
(2) Kang, N.; Xu, Y.-Z.; Wu, J.-G.; Feng, W.; Weng, S.-F.; Xu, D.-F. *Phys. Chem. Chem. Phys.* **2000**, *2*, 3627−3630.
(3) Lehman, S.; Wagener, K.; Baugh, L.; Rucker, S.; Schulz, D.; Varma-Nair, M. *Macromolecules*, in press.
(4) Baughman, T.; Wagener, K. *Adv. Polym. Sci.* **2005**, *176*, 1−42.
(5) *Handbook of Metathesis;* Grubbs, R. H., Ed.; Wiley-VCH: New York, 2003; Vol. 3.
(6) (a) Hillmyer, M.; Laredo, W.; Grubbs, R. *Macromolecules* **1995**, *28*, 6311−6316. (b) Baughman, T. Ph.D. Thesis, University of Florida, Gainesville, FL, 2006.
(7) Baugh, L.; Lehman, S.; Wagener, K.; Schulz, D.; Berluche, E. U.S. Pat. Appl. Publ. 2005/0137369, June 23, 2005.
(8) Hopkins, T.; Wagener, K. *J. Mol. Catal. A: Chem.* **2004**, *213*, 93−99.
(9) Heiney, P. A. Datasqueeze: A Software Tool for Powder and Small-Angle X-Ray Diffraction Analysis. *Commission on Powder Diffraction Newsletter* **2005**, *32*, 9−11.
(10) (a) Otsuka, H.; Mori, K-i.; Endo, T. *Macromol. Rapid Commun.* **2001**, *22*, 1335−1339. (b) Otsuka, H.; Fujiwara, H.; Endo, T. *J. Polym. Sci., Part A: Polym. Chem.* **1999**, *37*, 4478−4482.
(11) Hagemann, H.; Strauss, H.; Snyder, R. *Macromolecules* **1987**, *20*, 2810−2819.
(12) Berda, E.; Baughman, T.; Wagener, K. *J. Polym. Sci., Part A: Polym. Chem.* **2006**, *44*, 4981−4989.
(13) Brandrup, J.; Immergut, E. H. *Polymer Handbook,* 3rd ed.; John Wiley and Sons: New York, 1989.
(14) McEvoy, R.; Krause, S.; Wu, P. *Polymer* **1998**, *39*, 5223−5239.
(15) Calculated using all-trans carbon−carbon bonds with 0.154 nm bond length and 120° bond angle.
(16) Boz, E.; Wagener, K.; Ghosal, A.; Fu, R.; Alamo, R. *Macromolecules* **2006**, *39*, 4437−4447.
(17) Lieser, G.; Wegner, G.; Smith, J.; Wagener, K. *Colloid Polym. Sci.* **2004**, *282*, 773−781.
(18) Brandrup, J.; Immergut, E. H. *Polymer Handbook,* 3rd ed.; John Wiley and Sons: New York, 1989.

MA070841R